Simulation of Refinery Catalyst Pore Structure from Mercury Porosimetry data using Porexpert

Dim P.E.[1]; Laudone G.M.[2]; Gribble C.M.[2]; Matthews G.P.[2] and Rigby S.P.[3]

[1]Department of Chemical Engineering, Federal University of Technology, Minna, Nigeria.
[2]School of Geography, Earth and Environmental Sciences, Plymouth University, Plymouth, UK
[3]Department of Chemical and Environmental Engineering, University of Nottingham, UK
Email: pevdim@yahoo.com, paul.dim@futminna.edu.ng

Abstract

The simulation of refinery catalyst using Porexpert software is reported. The pore structure modelling and simulation method is employed for estimating the pore properties of catalyst using a network model of void structure based on mercury intrusion porosimetry (MIP). First, the network model is made to reproduce the percolation behaviour by matching the simulated percolation characteristics to an experimental MIP curve. The method is applied to the catalyst samples, and a network is derived in which mercury intrusion curve, porosity, connectivity, pore and throat size distributions are obtained. The study revealed that the network model has three main characteristics: a real pore space geometry; the same geometry is used to model a wide range of properties, and no property-independent fitting parameters are invoked, and thus the method can be applied for analysis and correlation of the pore properties of porous media. The results suggest that the network model can be used to estimate the samples particle distributions and the permeability of the samples within similar order of magnitude.

Keywords: Pore, Simulation, Porosimetry, Porexpert, Catalyst, Permeability

Introduction

The characterisation of porous materials is a difficult task and this has being a challenge for over the years. However, a critique of the limitations of single-technique characterisations of the void space of porous media, and quantitative investigation of the additional information, which can be gained from a Cartesian void network model. The experimental samples are catalysts. It is convenient to categorise void space architecture into four levels. The primary structure of a porous material is taken to be the distribution of void sizes, the secondary structure is the connectivity of these voids, the tertiary is structure the relationship between the sizes of voids and the sizes of their immediate connecting neighbours, and the quaternary structure is the size auto-correlations and gradations over the sample as a whole. These different levels of structure contribute to important properties of the sample, such as its filtration efficiency and capacity (Price *et al*., 2009), absorption and wetting characteristics (Wallqvist *et al*., 2009), and the adsorption and diffusion of pore fluids (Charlotte *et al*., 2015; Landone *et al*., 2010). The quaternary structure determines the anisotropy of these characteristics relative to the direction of application or flow of fluids (Gribble *et al.*, 2011).

Catalyst deactivation by coke deposition has been identified as one of the main challenges suffered by THAI-CAPRI process. Where "Toe-to-Heel Air Injection", is known as THAI, and Catalytic upgrading Process In-situ (CAPRI) is a way

to further enhance the heavy oil upgrading arising from the THAI process itself. Different techniques have been reported used to determine the pore structure of porous media. Nearly all methods suffer some drawback. Microscopy is one of the methods that gives a 2-dimensional view, with no information about the 3-dimensional connectivity of voids space. This connectivity is known to have a pronounced effect on properties such as the permeability, diffusion and trapping of pore fluids, and filtration characteristics (Charlotte *et al*., 2015, Landone *et al*., 2010). Microtoming on the other hand provided information layer by layer, but connections of voids between layers have to be inferred. Tomography is essentially characterised with a 3-dimensional mapping of the voids, but lack appreciable resolution to give all the interconnections (Laudone *et al.*, 2015, Gribble *et al.,* 2011). Porexpert is designed to bring all this partial information together, by constructing a realistic simulation of porous material (Laudone *et al*., 2014, 2015, Charlotte *et al*., 2015). Porexpert is a software package which allows the study of the pore level properties of any mesoporous or macroporous solid, i.e. a solid with pore sizes greater than 2 nm (Thommes, 2010). These make it most suitable since catalyst deactivation does not only depend largely on pores and pores structure but also take place in the pores. In fact, deactivation is typically more rapid in porous media having small pores or apertures and /or mono-dimensional structure (Guisnet and Magnoux, 1989). The generated network structures created by the software are constructed under the criterion that they hold the same percolation characteristics as those derived from experimental data. Therefore in this study Porexpert software will be used to characterise candidate catalyst used in the process, by modelling and simulation of the experimental data obtained from Mercury Porosimetry experiment.

Materials and Methods

Materials

The catalyst samples studied in this work were Ketjenfine hydroprocessing catalysts-NiMo type (Extrudates & Fragment) and CoMo type, which were referred to as samples A, B & C. The samples contained, respectively, Precipitated silica: < 10; Nickel (II) oxide: < 10; Molybdenum (VI) oxide: < 30; Phosphorus pentoxide: 0-9; Aluminium oxide: balance (w/w %) and Precipitated silica: 0-6; Cobalt (II) oxide: 1-10, Molybdenum (VI) oxide: <25; Phosphorus pentoxide: 0-4; Aluminium oxide: balance (w/w%) of particles with diameter ~1 mm and with a length of ~7 mm.

Methods

Mercury porosimetry determination of properties

Mercury porosimetry was performed on a Micrometrics Autopore IV 9500 mercury porosimeter (Micrometrics Corporation, USA) with a pressure range from 0.01 to 414 MPa, following ISO9001 : 2008 protocols. The standard equilibration time used for each pressure point was 30 s. The sample was first evacuated to a pressure of ~50 µm Hg in order to remove physisorbed water from the interior of the sample. The raw data were analyzed according to the Washburn equation the value taken for the surface tension of mercury was 0.485 Nm^{-1}. The corresponding values for the advancing and receding contact angles were both taken as 130^{O}. The pressure values were converted into pore diameters using the Laplace equation. The pore diameter was

subsequently plotted against intruded volume to give a volumetric distribution of pore size curve.

Simulation of MIP data

The three catalyst samples from MIP experiment were modelled in this work using Porexpert software. The experimental data is fitted using an iterative fitting of pore and a throat size until a "closest fit" is found. The fitting process is undertaken using an annealed simplex algorithm, which works to find the global minima for a five dimensional surface (Matthews *et al.*, 2010). To simulate mercury intrusion a computational representation of fluid is applied to the top face (maximum z) of the unit cell only, and percolates in the –z direction. The throat skew, throat spread, pore skew, connectivity and short range size auto correlation are adjusted by the Boltzmann-annealed amoeboid simplex (Johnson *et al*., 2003) to give a close fit to the entire mercury intrusion curve. 3D void networks are generated by stochastically creating unit cells comprising an array of 1000 (10×10×10) cubic pores connected by up to 3000 cylindrical throats (Fig. 1). The network model 'Pore-Cor' has been previously used to model a range of materials such as soil, sandstone, catalysts, limestone and paper coating (Landone *et al*., 2013, 2015, Bodurtha *et al*., 2005). The network simulator has been used as a predictive tool for the study of absorption in compacted mineral blocks (Ridgway *et al.*, 2001) modelling diffusion in porous structure (Laudone *et al*., 2010). It represents the void structure of porous medium as a series of identical interconnected unit cells with periodic boundary conditions. Each unit cell comprises an array of 1000 nodes in a cubic-close-packed array equally spaced at a distance from each other in each cartesian direction. Cubic pores are positioned with their centres at each node and are connected by cylindrical throats in each cartesian direction. The pores are of 100 discrete sizes distributed equally over a logarithmic scale (Laudone *et al*., 2008).

Results and Discussion

Sample A, structure shown in Figure 1 has simulated porosity of 55.86 % and experimental porosity of 55.84 %, respectively. It has a unit cell length of 3.139 µm and structure side length of 3139 µm in x, y and z direction. The Porexpert network simulation software also modelled correctly the trend of the experimental mercury intrusion curve for samples B and C. The fits between the experimental and simulated curve matched very closely. The sample B structure shown in Fig. 1 has simulated porosity of 60.39 % and experimental porosity of 60.40 %, respectively. It also has a unit cell length of 1.34 µm and structure side length of 1349 µm in x, y and z direction. While structure of sample C shown in Figure 1, have simulated porosity of 37.87 % and experimental porosity of 37.87 %, respectively. It has a unit cell length of 0.348 µm and structure side length of 348 µm in x, y and z direction. Comparing the experimental and simulated curve of samples, it can be seen that in the mesopore size range, the pore size distributions have an overall sigma shape with relatively flat plateaus at both small and very large pore sizes. In this simulation, mercury is injected normal to the xy plane at z= 0 in the -z direction. Since the unit cell repeats in each direction, z = 0 at z =I_{cell}, the unit cell size, and the injection corresponds to intrusion downwards from the top surface (Fig. 1). Therefore the generated structures

presented in this study are the result of mapping the mercury intrusion curve of the sample onto a network of pores and throats.

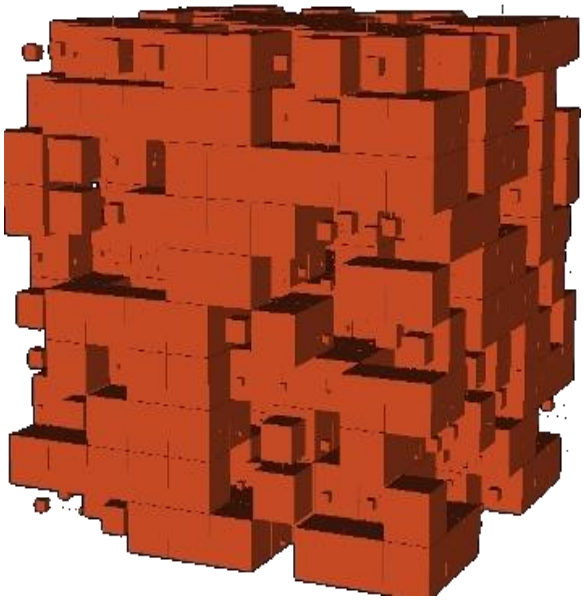

(a)

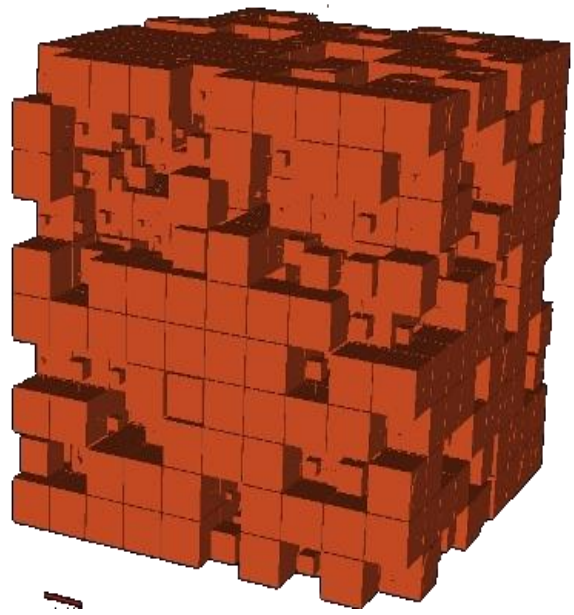

(b)

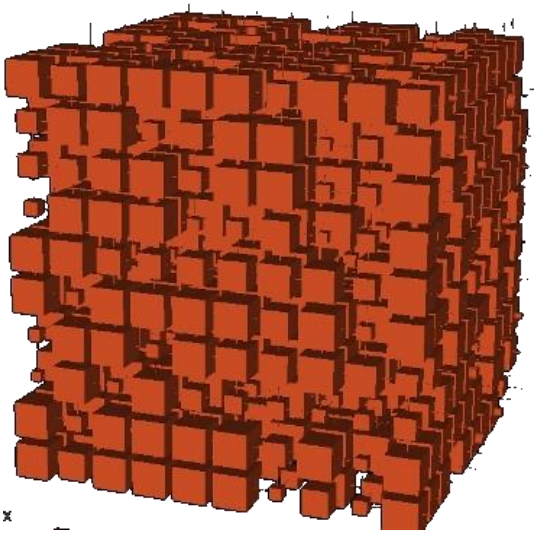

(c)

Fig. 1: (a) Sample A; (b) Sample B; and (c) Sample C

The experimental mercury porosimetry curve was fitted using iterative trials of pore and throat sizes, and the structure which gives the closest match to the intrusion curve chosen. The fitting process was undertaken using an annealed simplex algorithm which works to find the global minimum for a five dimensional global minimum (Matthews *et al*., 1993). The fits between the experimental and simulated curve matched very closely as shown in Fig. 2.

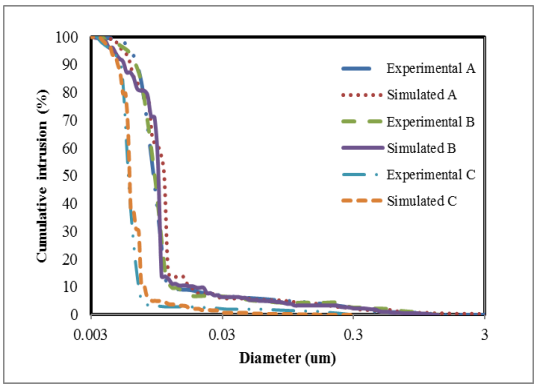

Fig. 2: Comparison of experimental and simulated mercury intrusion curve of samples**.**

The analysis representation of the connectivity distributions of all the samples is shown in Fig. 3. The connectivity

distributions of all the pores within the unit cell determines how many throats are connected to each individual pore. There is similarity in the shape of the paths of A and B distribution curves. This could suggest that fragmentation of A and B (powder) had a negligible effect. The three samples have highest connectivity value of six. It can be seen from Figure 3 that connectivity distribution curves for sample C differs with no peak present. This could also suggest that sample C may have connectivity higher than 6.

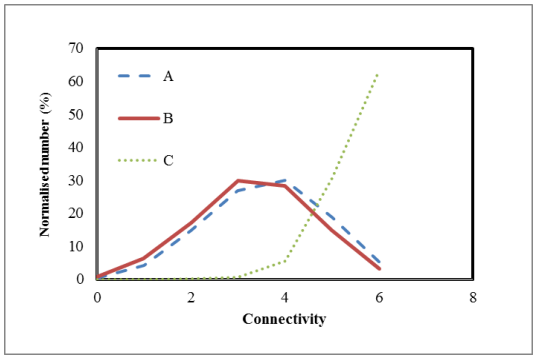

Fig. 3: Connectivity distribution of catalyst samples

Fig. 4 shows pore and throat size distribution of the simulated catalyst samples. The positions of the pores and throats are random, determined by a pseudorandom number generator. Their distributions are characterized by peaks. There is possibility that the connectivity distribution curve for C may have increased further, but stopped by what could be believed to be an artefact from the software.

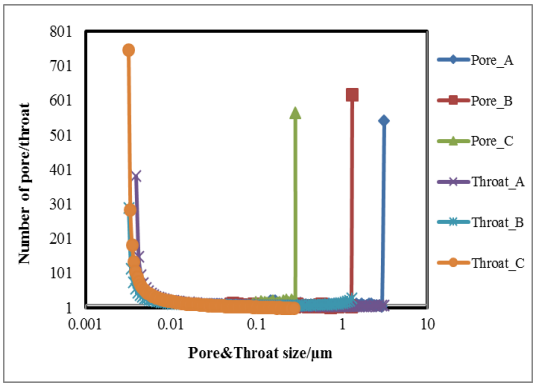

Fig. 4: Pore and throat size distribution of catalyst samples

The connectivity distribution tells whether a pore has zero connectivity that is an isolated pore, one connection that is an ink bottle pore, two connections, three connections, four connections, five connections and six connections. It is worth mentioning that for all connectivity distribution present in the sample, the ink bottle pores, which are the pores with one connection, known to be the most important because these pores are mainly responsible for the hysteresis of mercury during a mercury porosimetry experiment. The simulated void structures generated for this samples show different particle size distribution. In order to generate the correct features in the void network, the pores and throat size distribution are arranged or packed, such that the sizes of the largest pore and throat all accumulate at minimum and maximum size for pores and throat, respectively. It can be seen that sample B has the highest number of pores (Fig. 4 and Table 1), followed by A and C. Conversely sample C which has the smallest number of pores, displayed higher throat number than A and B which both have the same throat number. The effective thermal conductivity, porosity, number of pores and throat of the simulated network structures are presented in Table 1. These represents the features of

the catalyst samples as simulated by the software.

Table 1: Conductivity, porosity and number of pores and throat of simulated network structure

Sample	Porosity %	Pore	Throat	Pore conductivity (W/mK)	Solid Conductivity (W/mK)	Permeability (mD)
A	55.86	46	99	0.0694	0.888	2.32E-08
B	60.39	55	99	0.061	0.792	5.33E-08
C	37.87	31	97	0.25	0.758	3.67E-07

The permeability results as modelled using Porexpert are shown in Table 1. The predicted permeability of sample A and B are of similar order of magnitude. However, sample B showed a higher permeability values than sample A. This can be seen clearly in Table 1. This could be supported by the fact that B is the fragmented form of A. Considering the entire catalyst sample in their various forms they displayed a unique features and characteristics in the pores, throat, connectivity distribution and fitting parameters. This method of permeability calculation employed in this work is a more precise approximation than the other main methods of solving the flow in void networks, namely the resistor network (Martins *et al*., 2007) and effective medium approximations (Stamatakis and Tien, 1988; Berg, 1995). Permeability is the most important property of a porous medium. It describes the conductivity of a porous medium with respect to fluid flow. Permeability describes how easily a fluid is able to move through porous material. It is related to the connectedness of the void spaces and to the pores sizes of the sample. The network simulator can also calculate the permeability of the simulated porous structures using equation (1)**.** It is assumed that the flow of liquid through the network is laminar, and so obeys Poiseuille's equation. Combining Poiseuille's equation with the Darcy equation results in an expression for the Darcy permeability independent of the pressure gradient imposed on the sample (Matthews *et al*., 1993; Bodurtha *et al*., 2005).

$$K = \frac{\pi}{8} \underset{cell}{\Omega}\left(F_{arcs}\right) \frac{l_{cell}}{A_{cell}} \qquad (1)$$

where k is absolute permeability, l_{cell} is the length of the unit cell of the network model, and A_{cell} is the cell's cross-sectional area. A network analysis approach to this problem supplies the term $\underset{cell}{\Omega}(F_{arcs})$ as the maximal flow capacity through the network of pores and throats (Matthews *et al*., 1993). It is calculated by means of the archetypal network capacity algorithm developed by Dinic (Ahuja *et al.*, 1997). There is an overall conservation of flow, so that the entire volume of fluid entering the top of the unit cell emerges at the bottom, with no build-up through the network. The value obtained, as the maximal flow, is based on the capacities of only the channels found to carry flow. The solution derived is analogous to the ‘‘trickle flow’’ of an incompressible fluid, which finds various tracks through the unit cell in the _x, _y, and _z, directions.

Conclusions

The pore network simulation method for estimating the pore properties of refinery catalyst using a network model of void structure based on mercury intrusion porosimetry (MIP) was also carried out. The study revealed that the network model has three main characteristics: a real pore space geometry; the same geometry is used to model a wide range of properties, and no property-independent fitting parameters are invoked, and thus the method can be applied for analysis and correlation of the

pore properties of any porous media. The results suggest that the network model can be used to estimate samples particle distributions and it also successfully modelled the permeability of the samples to within similar order of magnitude.

Acknowledgement

The authors wish to acknowledge Prof P Matthews (University of Plymouth, UK) for the provision and support with the use of POREXPERT software package.

References

Ahuja, R. K.; Kodialam, M.; Mishra, A. K. and Orlin, J. B. (1997). Computational investigations of maximum flow algorithms. *European Journal of Operational Research*, Vol. 97, 509-542.

Berg, C.R. (1995). A Simple, Effective-Medium Model For Water Saturation In Porous Rocks. *Geophysics*, Vol. 60, 1070-1080

Bodurtha, P. A.; Matthews, G.P.; Kettle, J. P. and Roy, L. M. (2005). Influence of anisotropy on the dynamic wetting and permeation of paper coatings. *Journal of Colloid and Interface Science*, Vol. 283, 171-189.

Charlotte, L. Levy, G. Peter Matthews, Giuliano M. Laudone, Christopher M. Gribble, Andrew Turner, Cathy J. Ridgway, Daniel E. Gerard, Joachim Schoelkopf, and Patrick A. C. Gane. (2015). Diffusion and Tortuosity in Porous Functionalized Calcium Carbonate. *Industrial & Engineering Chemistry Research*, Vol. 54, No. 41, 9938-9947

Gribble, C. M.; Matthews, G.P.; Laudone, G. M., Turner, A.; Ridgway, C. J.; Schoelkopf, J. and Gane, P.A.C. (2011). Porosimetry, image analysis and void network modelling in the study of the pore-level properties of filters.*Chemical Engineering Science*, Vol. 66, 3701-3709.

Guisnet, M. and Magnoux, P. (1989). Coking and Deactivation of Zeolites–Influence of the Pore Structure. *Applied Catalysis*, Vol. 54, 1-27.

Johnson, A.; Roy, I.M.; Matthews, G.P. and Patel, D. (2003). An Improved Simulation of Void Structure, Water Retention and Hydraulic Conductivity In Soil With The Pore-Cor Three-Dimensional Network. *European Journal of Soil Science*, Vol. 54, 477- 489.

Laudone, G.M.; Matthews, G.P. and Gane, P.A.C. (2008). Modelling diffusion from simulated porous structures. *Chemical Engineering Science*, Vol. 63, 1987-1996.

Laudone, G. M.; Matthews, G.P. and Gane, P.A.C. (2010). Modelling Diffusion from Simulated Porous Structures. *Chemical Engineering Science*, Vol. 63, 1987-1996.

Laudone, G. M.; Christopher M Gribble; Katie L Jones; Hannah J Collier and G Peter Matthews, (2015). Validated a priori calculation of tortuosity in porous materials including sandstone and limestone.*Chemical Engineering Science*, Vol. 131, 109-117

Laudone, G.M; Christopher M. Gribble, G. Peter Matthews (2014). Characterisation of the porous

structure of Gilsocarbon graphite using pycnometry, cyclic porosimetry and void-network modelling. *C A R B ON*. Vol. 7, No. 3, 61 –70

Matthews, G.P.; Laudone, G.M.; Gregory, A.S.; Bird, N. R.A.; Matthews, A.G. and Whalley, W. R. (2010). Measurement and Simulation of the Effect of Compaction on the Pore Structure and Saturated Hydraulic Conductivity of Grassland and Arable Soil. *Water Resources Research*, Vol. 46, 455-462

Matthews, G.P.; Moss, A.K.; Spearing, M.C., and Voland, F. (1993). Network Calculation Of Mercury Intrusion and Absolute Permeability In Sandstone and other Porous-Media. *Powder Technology*,Vol. 76, 95-107.

Ridgway, C.J.; Schoelkopf, J.; Matthews, G.P.; Gane, P.A.C. and James, P.W. (2001). The Effects of Void Geometry and Contact Angle on the Absorption of Liquids Into Porous Calcium Carbonate Structures. *Journal of Colloid and Interface Science*, Vol. 239, 417-431.

Thommes, M. (2010).Physical Adsorption Characterisation of Nanoporous Materials. *Chemie Ingenieur Technik*, Vol. 82, 1059 – 1071.

Price, J.C.; Matthews, G.P.; Quinlan, K.; Sexton, J. and Matthews, A.G.D.G. (2009). A Depth Filtration Model of Straining Within the Void Networks of Stainless Steel Filters. *AIChE Journal*, Vol. 55, 3134-3144.

Wallqvist, V.; Claesson, P.M.; Swerin, A.; O□Stlund, C.; Schoelkopf, J. and Gane, P.A.C. (2009). Influence of Surface Topography on Adhesive and Long-Range Capillary Forces Between Hydrophobic Surfaces in Water. *Langmuir*, Vol. 25, 9197-9207.

Stamatakis, K. and Tien, C. (1988). Dynamics of Batch Sedimentation of Polydispersed Suspensions. *Powder Tech*, Vol. 56, 105-117

Martins, A. A.; Laranjeira, P.E.; Lopes, J.C.B. and Dias, M.M. (2007). Network Modeling of Flow In A Packed Bed. *Aiche Journal*, Vol. 53, 91-107